

GaAs-(Ga, Al)As double quantum rings: confinement and magnetic field effects

This article has been downloaded from IOPscience. Please scroll down to see the full text article.

2008 J. Phys.: Condens. Matter 20 285215

(<http://iopscience.iop.org/0953-8984/20/28/285215>)

View [the table of contents for this issue](#), or go to the [journal homepage](#) for more

Download details:

IP Address: 129.252.86.83

The article was downloaded on 29/05/2010 at 13:32

Please note that [terms and conditions apply](#).

GaAs–(Ga, Al)As double quantum rings: confinement and magnetic field effects

F J Culchac^{1,2}, N Porrás-Montenegro^{1,3} and A Latgé²

¹ Department of Physics, Universidad del Valle, AA 25.360, Cali, Colombia

² Instituto de Física, Universidade Federal Fluminense, 24210-340, Niterói-RJ, Brazil

³ Instituto de Física, Universidade Estadual de Campinas—UNICAMP, CP 6165, Campinas—SP, 13083-970, Brazil

E-mail: latge@if.uff.br

Received 14 March 2008, in final form 29 May 2008

Published 17 June 2008

Online at stacks.iop.org/JPhysCM/20/285215

Abstract

Here we address a theoretical study of concentric GaAs–(Ga, Al)As double quantum rings, under a magnetic field applied perpendicularly to the ring plane. Electron–hole transition energies are calculated as a function of the system geometry confinement, following a single-particle picture, neglecting interaction effects. We adopted an effective-mass approximation, within a hard potential model calculation, exactly solved by using confluent hypergeometric functions. A huge dependence on the barrier width value and on the external ring width of the Ga_{1-x}Al_xAs coupled rings is found for the transition energy values. The results show a high competition between geometric and magnetic-field confinement, leading to an increase of the electron–hole energies with the magnetic field, and a reducing behavior as the outer ring width is assumed to be larger. Our results are in quite good agreement with the experimental data by Mano *et al* (2005 *Nano Lett.* **5** 425).

(Some figures in this article are in colour only in the electronic version)

1. Introduction

Optical and transport properties in semiconductor low dimensional systems crucially depend on the quantum confinement suffered by the charge carriers in the structures. This has been a challenge, due to the novel physics properties and their potential technological application. Nanostructures like quantum wells (QWs), well wires (QWWs), dots (QDs) and rings (QRs) have been grown by several methods, such as self-assembly techniques. QDs, for instance, have been theoretically studied taking into account one and several electrons confined, and under different probes such as applied electric and magnetic fields [1]. The effects of the geometric confinement on the exciton binding energy, the electron–hole separation and the linear optical properties have been some of the physical properties investigated [2]. A great difference between quantum rings and dots is concerned with their topology due to the central hole of the former. More explicitly, a QR offers the possibility of trapping a magnetic flux in its interior, allowing new interesting quantum phenomena, such as the Aharonov–Bohm (AB) effects [3]. Anisotropic rings are also studied in the presence of external fields [4, 5].

Different spectroscopic techniques have been used to examine the ground and excited states of confined electrons in QRs. Important reported evidence is the occurrence of a transition in the electron ground state from angular momentum $l = 0$ to -1 , when a magnetic field is applied in the interior of the ring [6, 7]. Considering Coulomb correlations, the excitonic AB effect exists in finite ring width. When the ring width becomes large the AB effects are suppressed [8]. Concentric double quantum rings (DQRs) have also been considered as a natural candidate for exhibiting interesting physical responses [9, 10]. Mano *et al* [11, 12] reported growth results of GaAs–GaAlAs DQRs by adopting droplet-epitaxial techniques and micro-photoluminescence measurements. They were able to determine the electronic structure and the electron–heavy-hole optical transitions, in the absence of magnetic fields. Model calculations based on parabolic confinement potentials and exact diagonalization techniques were addressed to study the quantum confined double ring structures under applied magnetic fields [13]. Modifications of the periodicity of the Aharonov–Bohm oscillations were predicted. Interesting studies on excitons in ideal double quantum ring systems under magnetic fluxes lead one to address the possibility of switching

between bright exciton ground states and novel dark states with nearly infinite lifetimes [14]. Climente *et al* [15], using the local spin density approximation, found that the energy structure in the low lying energy states is essentially modulated by the inter-ring barrier distance, and the energy structure is essentially that of an isolated SQR. Quite recently, the effects of Coulomb impurities in the Aharonov–Bohm effects in these DQR structures have also been addressed [16].

Motivated by presenting a simple theoretical description of the main experimental data [11] on DQRs we report here a theoretical analysis of the effects of the geometry and magnetic confinement on the electron, light- and heavy-hole ground-state energies in concentric GaAs–Ga_{0.7}Al_{0.3}As double quantum rings. Rather than using a parabolic potential [13] as used previously to describe the particle (electron and hole) confinements, we adopt a hard potential which is more adequate to describe the experimental potential profile of the annular structure grown by Mano’s group [11]. Electron–heavy- and light-hole transition energies in QRs are also discussed. We believe that these new nanostructured ring materials are particular suitable to exhibit interesting quantum size phenomena due to the robust electron and hole confinements in such circular geometries, that may be even enhanced as a function of the particular characteristic lengths presented. One example should be the increasing of optical transition channels allowed by the great number of quantum states. We may also wonder about challenging applications as a consequence of multiple periods of the Aharonov–Bohm oscillations.

2. Theory

We consider a concentric GaAs–Ga_{0.7}Al_{0.3}As DQR, composed of an internal ring with radii ρ_A and ρ_B , an external one with radii ρ_C and ρ_D , and a confinement length H in the z -direction, subjected to a magnetic field perpendicular to the plane of the ring. The Hamiltonian of an electron in the effective-mass approximation is written as

$$H = \frac{1}{2m_e^*}(\mathbf{P} + e\mathbf{A}/c)^2 + V(\rho, z), \quad (1)$$

where m_e^* is the electron effective mass, \mathbf{A} is the vector potential of the magnetic field, and $V(\rho, z)$ is the confinement potential in the radial and z -direction. For a uniform magnetic field the vector potential can be written as $A(\rho) = 1/2Bx\rho$, with $\mathbf{B} = B\hat{e}_z$, whose components in cylindrical coordinates become $A_\rho = A_z = 0$ and $A_\phi = 1/2B\rho$. The finite radial confinement potential is given by

$$\begin{aligned} V_b(\rho) &= V_c & \rho < \rho_A, & \quad \rho_B < \rho < \rho_C, & \quad \text{and} & \quad \rho > \rho_D \\ V_b(\rho) &= 0 & \rho_A < \rho < \rho_B & \quad \text{and} & \quad \rho_C < \rho < \rho_D, \end{aligned} \quad (2)$$

while in the z -direction $V(z) = V_c$ for $|z| \geq H/2$, and zero elsewhere. The Schrodinger equation may be written in cylindrical coordinates as

$$\begin{aligned} -\frac{\hbar^2}{2m_e^*} \left(\frac{\partial^2 \Psi}{\partial \rho^2} + \frac{1}{\rho} \frac{\partial \Psi}{\partial \rho} + \frac{1}{\rho^2} \frac{\partial^2 \Psi}{\partial \phi^2} + \frac{\partial^2 \Psi}{\partial z^2} \right) - \frac{i\hbar\omega_c}{2} \frac{\partial \Psi}{\partial \phi} \\ + 1/8m_e^*\omega_c^2\rho^2\Psi + [V_b(\rho, z) - E]\Psi = 0 \end{aligned} \quad (3)$$

with $\omega_c = eB/m_e^*c$ being the electron cyclotron frequency. For the light- and heavy-hole carriers, the same Hamiltonian is used but considering the respective effective masses and charge signs. Electron and hole eigenvalue problems are solved in detail in [18]. Due to the axial symmetry one gets a confluent hypergeometric equation for the radial part of the wavefunction,

$$x\omega''_{n,l}(x) + (b-x)\omega'_{n,l}(x) - a\omega_{n,l}(x) = 0 \quad (4)$$

with $x = m^*w_c\rho^2/2\hbar$, $a = |l|/2 + 1/2 + l/2 - E/\hbar\omega_c$ and $b = |l| + 1$, n and l being the main and angular momentum numbers, respectively. The solution of equation (4) is given by a linear combination of confluent hypergeometric functions [18]

$$w_{n,l}(x) = AF_{n,l}(a, b, x) + BU_{n,l}(a, b, x). \quad (5)$$

In what follows, we have considered the conduction and valence band edges as the reference levels for the electron and hole energies, respectively, and have considered the case of $n = 0$. In the calculation of the transition energies we use

$$E_{ij} = E_g^{\text{GaAs}} + |E_i^C| + |E_j^V|, \quad (6)$$

with E_g^{GaAs} being the GaAs band gap energy (1.5194 eV) and E_i^C and E_j^V the electron and hole energies, respectively, regarding to the corresponding band edges. The electron GaAs effective mass is taken as $0.067 m_0$, and the corresponding light- and heavy-hole masses [11, 17] as $0.082 m_0$ and $0.51 m_0$, respectively.

With the purpose of investigating the effects of the geometrical details of the double ring nanostructures on the energy spectra, we consider different width values for the internal and external rings, $L_A = \rho_B - \rho_A$ and $L_C = \rho_D - \rho_C$, respectively, and also for the barrier width, $L_B = \rho_C - \rho_B$. On the other hand, fixed values for the internal radius ($\rho_A = 20$ nm) and width H (4 nm in the z -direction) have been considered for all DQRs studied. The choices of the DQR size parameters have been guided by self-assembled rings grown by the epitaxial method [11].

3. Results and discussion

To analyze the effects of magnetic and confinement effects on the energy spectrum of DQRs it is important to visualize how the energy for each angular momentum, l , evolves with the intensity of the magnetic field. This is illustrated in figure 1, for $l = -4, -3, \dots, 3, 4$, for electrons (top panel) and heavy and light holes (middle and bottom panels, respectively). One clearly notices that, similarly to the case of a single quantum ring [19], as the magnetic field is turned on, the angular momentum of the particle ground state changes from $l = 0$, in the null field case, to different values of l of which the signal depends on the particle nature (electron or holes) and field values, as expected.

Electron energies of GaAs–Ga_{0.7}Al_{0.3}As DQRs as a function of the outer ring width (L_C) are shown in figure 2, for different magnetic field intensities: $B = 0$ in symbols, 5 T in solid lines, and $B = 10$ T in thin lines. Two groups of

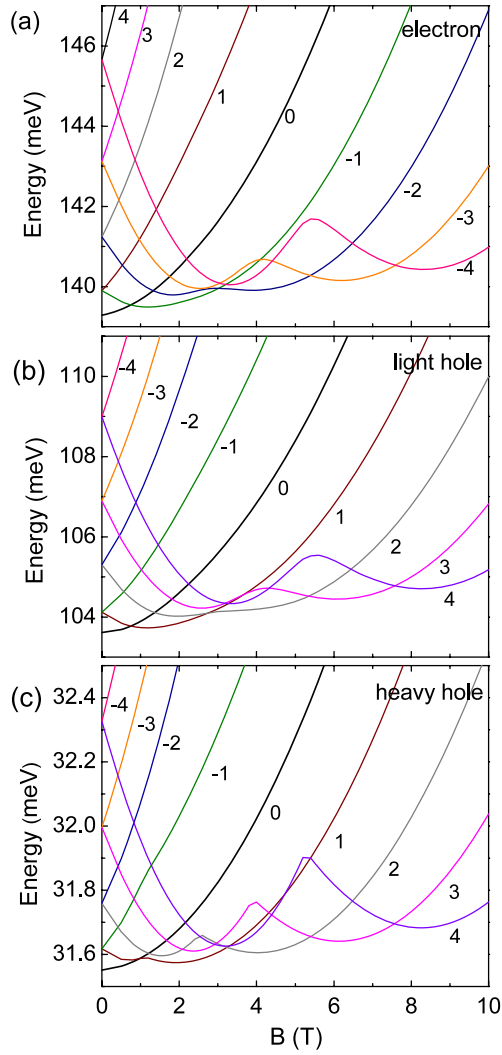


Figure 1. Energy spectra of (a) electron, (b) light hole and (c) heavy hole as functions of the magnetic field for a GaAs–Ga_{0.7}Al_{0.3}As DQR with $L_A = L_C = 10$ nm, $L_B = 5$ nm, and for angular momentum l varying from -4 to 4 .

DQR structures are considered, regarding the intensity of the tunnel coupling regime: those rings strongly coupled with a thin barrier width $L_B = 1$ nm shown in figure 2(a) and those belonging to a weak regime with $L_B = 5$ nm, figure 2(b). We have presented results for different angular momenta. The role played by the geometric and magnetic confinements, and their competition, is quite apparent.

One may notice that for zero magnetic field, $B = 0$ T, all energies are l degenerate and the ground state corresponds to $n = l = 0$, independent of the sizes of the DQRs. For L_C equal to or smaller than the inner ring (10 nm), the electron is confined in the inner ring and the $l = 0$ ground-state energy is quite close to that of a particle in a single QR. On the other hand, when the outer ring width is larger than the width of the inner one, the probability of finding the carrier in the external ring increases, and its energy diminishes. When a magnetic field is turned on, the extra confinement due to the cyclotron radius leads to an energy increase. As a consequence, one may expect an increasing in the critical outer-ring-width

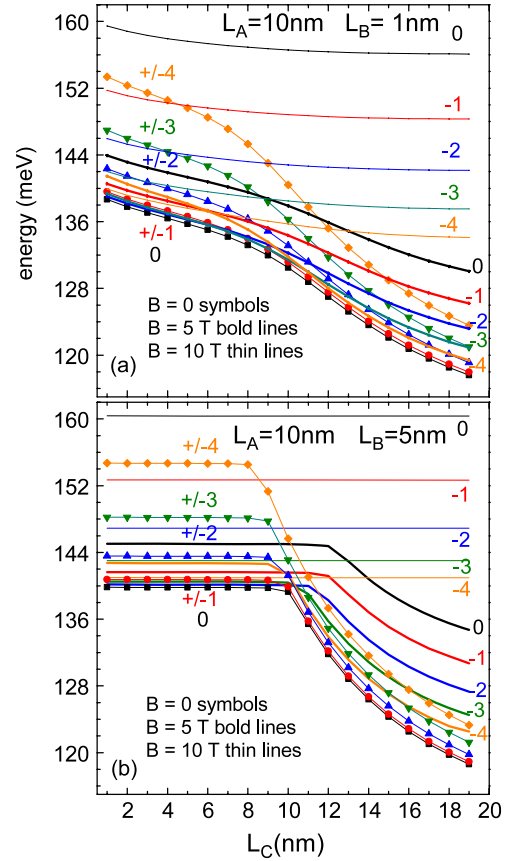


Figure 2. Electron energies of GaAs–Ga_{0.7}Al_{0.3}As DQRs as a function of the outer ring width for different magnetic fields: symbol curves are for null field, bold and thin lines are for $B = 5$ and 10 T, respectively. The internal ring length is $L_A = 10$ nm and the barrier width, L_B , is (a) 1 nm and (b) 5 nm.

value for which the state from the inner to the external ring takes place. This fact may be seen in figure 2(b) (bold lines) in the case of $B = 5$ T and weak tunnel coupling regime, for which the electron is located in the inner ring for L_C up to 10 – 12 nm, depending on the angular momentum. For $B = 5$ T the fundamental energy corresponds to an $l = -2$ state whenever $L_C < L_A$ ($L_B = 5$ nm). However, for DQRs with outer ring length $L_C > L_A$, lower l values are found for the electron ground state. For higher magnetic fields the particle is confined in the inner ring and the energy no longer depends on the size of the external ring. For the strong tunnel coupling regime, $L_B = 1$ nm, the particle tunnels more easily to the external ring and the probabilities of finding it in each ring are approximately the same. The energy increases with the magnetic field, but diminishes with the width of the outer ring for different angular momenta and null field. In the high magnetic field regime ($B = 10$ T), the electron energy is found to be identical to the result of a single quantum ring, and does not depend on the size of the external ring. However, in this magnetic confinement range, the energy associated with each one of the angular momenta is much more spread out for a narrow barrier than in the case of $L_B = 5$ nm, presenting also lower l -dependent energies.

To highlight the role played by the DQR barrier width in the determination of the electron energies we show explicitly

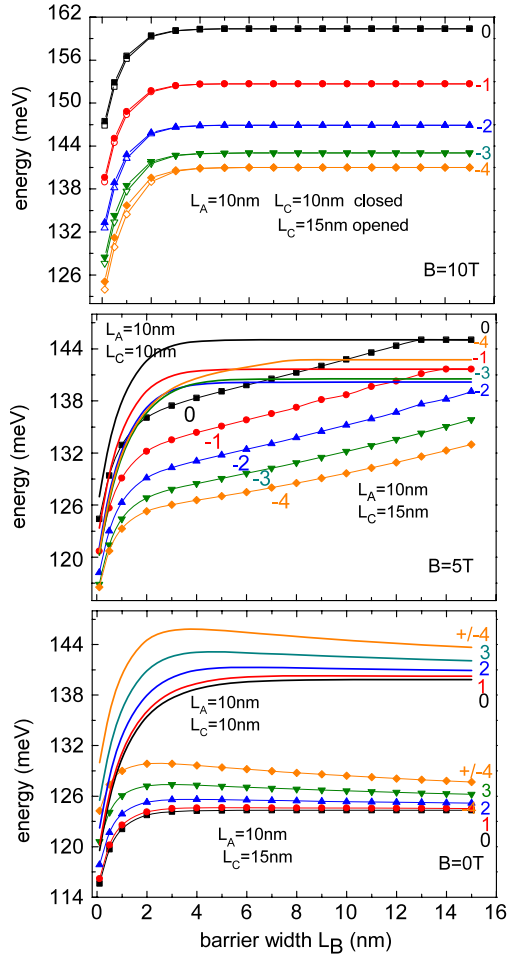


Figure 3. GaAs–Ga_{0.7}Al_{0.3}As DQR electron energy spectra for $l = -4, -3, -2, -1$ and 0 , as a function of the barrier width and for null field (upper panel) and $B = 5$ and 10 T (middle and low panel, respectively). Symbol curves are for $L_A = 10$ nm and $L_C = 15$ nm while continuous lines are for $L_A = L_C = 10$ nm.

in figure 3 the energy results as functions of the barrier size, for symmetric ($L_A = L_C$, continuous lines) and asymmetric ($L_A < L_C$, closed symbols) coupled ring structures. Different values of magnetic field are considered in the figures. For higher field values and increasing values of the barrier width, both the symmetric and asymmetric structures tend to the same energy values, for each one of the considered angular momenta l , as evidence of the strong magnetic confinement compared to the geometrical one. This is not the case for zero field, when a considerable energy difference is exhibited, for all l values and barrier widths. For intermediate B values one clearly gets competition between the confinement effects together with crossing between the curves belonging to different angular momenta, indicating that the ground state is quite dependent on the characteristic sizes of the double ring structure. Although our work is concerned with a single-particle approximation, our results for $B = 0$ coincide qualitatively well with those of a local spin density approximation study [15], where the energy spectrum is greatly modulated by the inter-ring distances (barrier).

A visualization of the electronic wavefunction within the ring structures helps one to understand the behavior of the

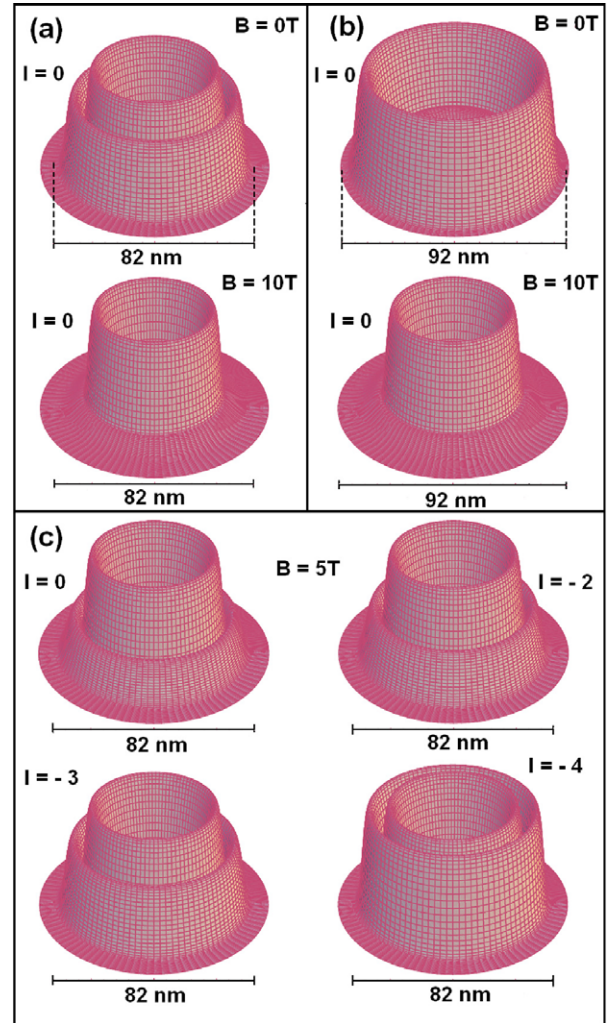


Figure 4. Probability amplitude of the electron state with $l = 0$ in a (a) symmetric ($L_A = L_C$) and (b) asymmetric ($L_A < L_C$) QDR for different magnetic fields. In both presented rings $\rho_A = 20$ nm, $L_A = 10$ nm, $L_B = 1$ nm, and the outer well widths are 10 and 15 nm in (a) and (b), respectively.

energy spectra. Two examples are displayed in figure 4 corresponding to GaAs–Ga_{0.7}Al_{0.3}As DQRs with $\rho_A = 20$ nm, $L_A = 10$ nm, $L_B = 1$ nm, and (a) $L_C = 10$ nm and (b) $L_C = 15$ nm. For the symmetric ring example (figure 4(a)), as the magnetic field increases the behavior of the carrier energy is similar to the corresponding single quantum ring energy. For the asymmetric case and $B = 0$ T, the probability density of the electron is higher in the wider ring than in the inner one, and the energy is approximately equal to that in a single ring of 15 nm in width. For increasing magnetic fields, it increases in the inner ring and in the limit of high magnetic confinement ($B = 10$ T) the charge distribution looks quite similar for symmetric and asymmetric DQRs, both exhibiting an electron localization in the internal ring. Consequently the carrier energies, for this particular $l = 0$ angular momentum, goes to the same value, as shown in figure 3. Of course, this is not a general result and depends on the coupling between the rings, given essentially by the barrier characteristic lengths and the diamagnetic confinement. Further, the dependence of

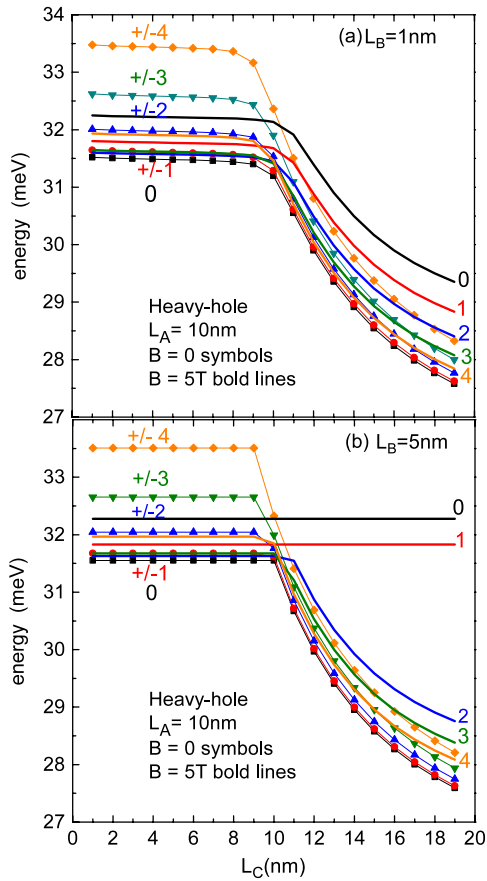


Figure 5. Heavy-hole energies of GaAs–Ga_{0.7}Al_{0.3}As DQRs for different angular momentum values (from 0 to 4), as a function of the width of the outer ring for null magnetic field (symbols) and $B = 5$ T (continuous curves), and barrier width of (a) 1 nm and (b) 5 nm.

the probability distribution on the angular momentum l , in the symmetric coupled ring structure, is shown in figure 4(c), for $B = 5$ T. One knows from figure 2 that for this structure and B value the ground state corresponds to $l = -2$. Actually, the corresponding electronic distribution is quite similar to the case of $l = 0$, but as l increases one clearly notices that the carrier may be also localized at the external ring.

To get the energy transitions from light- and heavy-hole states to the electronic one, we also calculate the corresponding hole states. The behaviors of the light-hole and electron energy spectra are quite similar due to the similarities of their effective masses. Results for the heavy-hole energy as a function of the outer ring width are shown in figure 5 for null field (symbols) and $B = 5$ T (bold lines).

Due to its larger effective mass, the heavy hole is more confined than the light one. The corresponding energies do not exhibit a noticeable variation with the size of the outer ring until it reaches a value greater than the internal ring, even for reduced between barrier width ($L_B = 1$ nm). The result reinforces the great localization nature of these carriers in the region of the inner ring. For configurations with $L_C > L_A$, the energies for all angular momenta considered start to drop. In the last case the heavy-hole probability amplitude extends in both the inner and outer rings, leading to a clear energy reduction as previously reported [15].

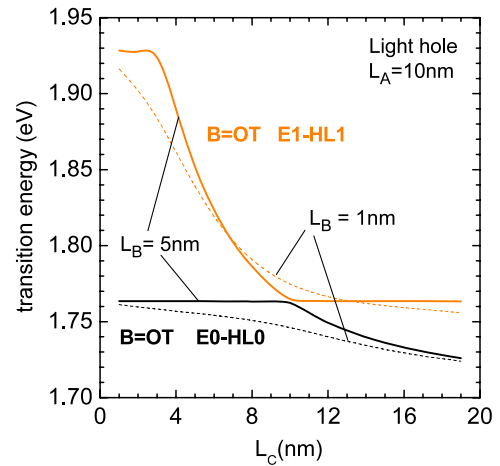


Figure 6. Light-hole–electron transition energies for $n = 0$ and $l = 0$ (E0–HL0) and $n = 1$ and $l = 0$ (E1–HL1) of a GaAs–Ga_{0.7}Al_{0.3}As DQR as a function of the width L_C of the outer ring for null magnetic field and barrier width equal to 5 nm (solid lines) and 1 nm (dotted lines).

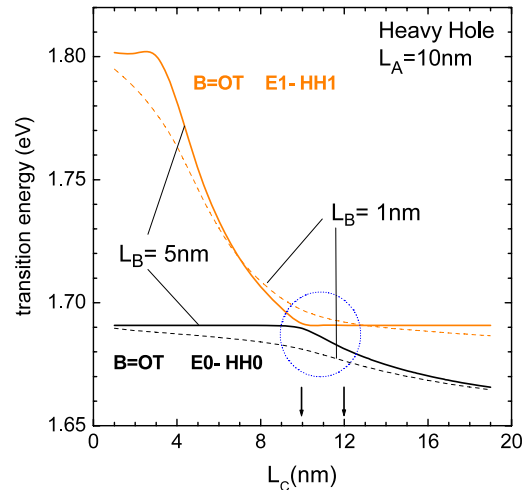


Figure 7. Heavy-hole–electron transition energies for $n = 0$ and $l = 0$ (E0–HH0) and $n = 1$ and $l = 0$ (E1–HH1) of a GaAs–Ga_{0.7}Al_{0.3}As DQR as a function of the width L_C of the outer ring for null magnetic field and barrier width equal to 5 nm (solid lines) and 1 nm (dotted lines).

Electron–hole transition energies are then calculated taking the case of null magnetic field and the states corresponding to $n = l = 0$, and $n = 1$ (second radial eigenvalue) and $l = 0$, named E0–HH0 and E1–HH1 and E0–LH0 and E1–LH1, for heavy and light holes, respectively. The results are shown in figures 6 and 7, as functions of the outer ring width. Two different values of the between barrier width, 5 and 1 nm, are considered. We have not presented the case of finite magnetic fields due to the complex changes in the angular momentum values as a function of the ring widths. A smaller barrier width contributes significantly to smooth the dependence of the transition energy value with the outer ring width due to the higher possibility of sweeping the material within both rings. Large barriers, as pointed out before, induce higher carrier localization within the inner ring.

As expected, the decreasing of the transition energies with the outer ring width follows the same trend as the electron and hole energies with these variations. A value of 1.69 eV for the electron–heavy hole transition energy has been found, for $B = 0$ (see figure 7), quite close to the experimental measurements reported by Mano [11], concerning a DQR system with approximately the same size [20] ($L_A = L_C = 10$ nm, and $L_B = 5$ nm).

One should notice that for outer ring widths between 10 and 12 nm, and for barrier widths in the range 1–5 nm, the E0–HH0 and E1–HH1 transition energies are between 1.68 and 1.7 meV, as indicated by the circle in figure 7. As previously reported [11], the main photoluminescence peaks corresponding to the electron–heavy-hole transitions are found in this energy range, more explicitly at 1.68 and 1.69 meV, associated with the E0–HH0 and E1–HH1 optical transitions. It can be observed that for symmetric rings, $L_A = L_C = 10$ nm and $L_B = 5$ nm, the E0–HH0 and E1–HH1 transition energies are very close, separated by approximately 1.5 meV, while for $L_C = 12$ nm the blue-shift in the transition energy is about 9.6 meV, reaching a value closer to the reported E1–HH1 energy transition, always in good agreement with experimental data [11]. Besides the neglected exciton interaction of our model calculation, the small differences with the experimental data may be related to the fact that the exact dimensions of the DQRs, such as the radii and height of the rings, are just approximately known. Actually, other possible electron-heavy- and light-hole recombination may be associated with further features in experimental data. For a proper calculation of inter-band absorption spectra a detailed analysis of the selection rules satisfied by the angular momentum must be considered [14]. As a consequence of the manifold quantum states provide by the enriched geometry of DQRs, a series of new findings in these nanostructures should be expected to have optical and transport applications.

Summing up, the present study on GaAs–(Ga, Al)As DQRs shows clearly the importance the characteristic geometric aspects of the nanostructured system (barrier and ring lengths) have in determining the energy spectra of the structures, fundamental for tuning desired resonances. The role of the barrier width and the difference between the widths of the inner and outer ring was found to be of crucial importance in determining the DQR spectra. Unequivocally, it was possible to identify the high competition between geometric and magnetic-field confinements. At high magnetic fields the electron–hole recombination is mainly present between

the two particles localized in the inner ring of the DQR. Of course, for a better quantitative analysis one should incorporate excitonic effects. Nevertheless, our present results for the electron–heavy-hole transition energies are in qualitatively good agreement with experimental data [11].

Acknowledgments

We thank the Colombian Scientific Agency Colciencias (Grant No 1106-05-13828) and Brazilian agencies CNPq, Instituto do Milênio, FAPERJ and FAPESP. AL is grateful for the hospitality of Universidad del Valle and NPM for the hospitality of Universidad Federal Fluminense and UNICAMP where part of this work was done.

References

- [1] Maksym P A and Chakraborty T 1990 *Phys. Rev. Lett.* **65** 108
- [2] Song J and Ulloa S E 1995 *Phys. Rev. B* **52** 9015
- [3] Aharonov Y and Bohm D 1959 *Phys. Rev.* **115** 485
- [4] Bruno-Alfonso A and Latgé A 2005 *Phys. Rev. B* **71** 125312
- [5] Bruno-Alfonso A and Latgé A 2008 *Phys. Rev. B* **77** 205303
- [6] Planelles J, Rajadell F and Climente J I 2007 *Nanotechnology* **18** 378402
- [7] Petroff P M, Lorker A and Imamoglu A 2001 *Phys. Today* **24** (May) 46
- [8] Lorke A, Luyken R J, Govorov A O, Kotthaus J P, Garcia J M and Petroff P M 2000 *Phys. Rev. Lett.* **84** 2223
- [9] Song J and Ulloa S E 2001 *Phys. Rev. B* **63** 125302
- [10] Malet F, Pi M, Barranco M, Lipparini E and Serra L I 2006 *Phys. Rev. B* **74** 193309
- [11] Muhle A, Wegscheider W and Haug R J 2007 *Appl. Phys. Lett.* **91** 133116
- [12] Mano T, Kuroda T, Sanguinetti S, Ochiai T, Tateno T, Kim J, Noda T, Kawabe M, Sakoda K, Kido G and Koguchi N 2005 *Nano Lett.* **5** 425
- [13] Kuroda T, Mano T, Ochiai T, Sanguinetti S, Sakoda K, Kido G and Koguchi N 2005 *Phys. Rev. B* **72** 205301
- [14] Szafran B and Peeters F M 2005 *Phys. Rev. B* **72** 155316
- [15] Govorov A O, Ulloa S E, Karrai K and Warburton R J 2002 *Phys. Rev. B* **66** 081309
- [16] Climente J I, Planelles J, Barranco M, Malet F and Pi M 2006 *Phys. Rev. B* **73** 235327
- [17] Chen G W, Chen Y N and Chuu D S 2008 *Solid State Commun.* **143** 515
- [18] Pavesi L and Guzzi M 1994 *J. Appl. Phys.* **75** 4779
- [19] Culchac F J, Porrás-Montenegro N, Granada J C and Latgé A 2008 *J. Microelectron.* **39** 402
- [20] Barticevic Z, Pacheco M and Latgé A 2000 *Phys. Rev. B* **62** 6963
- [21] Kuroda T 2007 private communication